Supplementary Material for: A probabilistic approach to characterizing drought using satellite gravimetry

Peyman Saemian[1], Mohammad J. Tourian[1], Omid Elmi[1]
Nico Sneeuw[1], Amir AghaKouchak[2,3]

[1]Institute of Geodesy, University of Stuttgart, Stuttgart, Germany
[1]Department of Civil and Environmental Engineering, University of California, Irvine, CA, USA.
[3]United Nations University Institute for Water, Environment and Health, Hamilton, Ontario, Canada

The supplementary material includes:

1. TWSA from GRACE observations
2. Long-term TWSA dataset
3. Handling trends
4. Major river basins
5. References

1 TWSA from GRACE observations

Two main approaches have been developed to process GRACE range-rate observations. In the first approach, the Earth's gravity field is parameterized using the global Spherical Harmonics (SHs) basis functions (see Wahr et al. (1998) for details). Within the past couple of years, an alternative approach for processing GRACE level 1 (L1) has been proposed which considers parameterizing with regional mass concentration functions (mascons) (Watkins et al., 2015a; Scanlon et al., 2016). In this study, we have used the latest version (version 2) of the Goddard Space Flight Center (GSFC) which can be accessed via `https://earth.gsfc.nasa.gov/geo/data/grace-mascons`. We have compared the uncertainty estimation from GSFC with the Jet Propulsion Laboratory (JPL) mas-

con solutions. The latest version (Release 6.1 Version 03) of the JPL mascon solutions used in the comparison can be obtained from `https://podaac.jpl.nasa.gov/dataset/TELLUS_GRAC-GRFO_MASCON_CRI_GRID_RL06.1_V3`. Moreover, we have compared the error estimation in the level-2 products, also known as formal errors, in Figure 1. Table S1 and Table S2 list all the mascons and level-2 products of GRACE and GRACE-FO used in this study, respectively.

Table S1. List of centers which provide Level-3 TWSA from GRACE and GRACE-FO.

Product	Sensor(s)	Source/Reference
GSFC v02 mascons	GRACE/GRACE-FO	Loomis et al. (2019)
JPL RL06.1 v03 L3 mascons	GRACE/GRACE-FO	Landerer et al. (2020); D. Wiese et al. (2018); Watkins et al. (2015b); D. N. Wiese et al. (2016)

The mascons products, like the one used in this study, estimate the uncertainty in the TWSA estimation, either in the form of spherical harmonics or global grids. Despite the same level-1 product, the errors in the mascons approaches vary among different centers, as they would use different processing approaches and background models. Figure S1 illustrates a spatio-temporal comparison comparison between two widely used mascons datasets, namely, JPL RL06-v02 and GSFC RL06-v02. the Figure S1 (a) shows the mean TWSA uncertainty from the above products from April 2002 to November 2022. The highest values belong to Greenland, the Amazonas, the Indian sub-continent, and the northwest of Canada. The Figure S1 (b) compares the time series of the global land averaged TWSA uncertainty from April 2002 to November 2022. The time series shows a sharp pick in 2015, followed by a positive trend related to the battery failure (Save, 2016; Mayer-Gürr et al., 2018; Bandikova et al., 2019). The two mascon solutions exhibit consistent uncertainty estimates ($\overline{\sigma} = 2.5\,\mathrm{cm}$) throughout the GRACE observation period, except for the initial year (April 2002 to June 2003). The elevated uncertainties in JPL solutions from April 2002 to June 2003, as well as at the last year of the GRACE-FO mission, stem from the application of a Kalman filter in the solution methodology, facilitating the temporal connection of adjacent months (D. Wiese et al., 2016). Notably, during the GRACE-FO mission, GSFC's uncertainty values are significantly higher ($\overline{\sigma} = 3.2\,\mathrm{cm}$ for GSFC compared to $\overline{\sigma} = 1.8\,\mathrm{cm}$ for JPL).

Table S2. List of GRACE(-FO) Level-2 solutions.

Center	Product	Sensor(s)	Time span
Solutions that include GRACE and GRACE-FO			
CSR	CSR RL06	GRACE	200204–201706
	CSR RL06	GRACE-FO	201806–present
GFZ	GFZ RL06	GRACE	200204–201706
	CSR RL06 (GFO)	GRACE-FO	201806–present
JPL	JPL RL06	GRACE	200204–201706
	CSR RL06 (GFO)	GRACE-FO	201806–present
ITSG	ITSG-Grace2018	GRACE	200204–201706
	ITSG-Grace_op	GRACE-FO	201806–present
LUH	LUH-Grace2018	GRACE	200301–201603
	LUH-GRACE-FO-2020	GRACE-FO	201806–present
COST-G**	Grace	GRACE	200204–201706
	Grace-FO	GRACE-FO	201806–present
AIUB	AIUB-RL02	GRACE	200302–201403
	AIUB-GRACE-FO_op	GRACE-FO	201806–present
CNES	CNES_GRGS_RL05	GRACE & GRACE-FO	200209–present
Solutions that include only GRACE			
Tongji	Tongji-Grace2018	GRACE	200204–201608
HUST	HUST-Grace2020	GRACE	200301–201607
IGG	IGG-RL01	GRACE	200204–201607
SWJTU	SWJTU-GRACE-RL01	GRACE	200303–201110
SWPU	SWPU-GRACE2021	GRACE	200204–201705
WHU	WHU RL01	GRACE	200204–201607
XISM&SSTC	GRACE01	GRACE	200204-201603

2 Long-term TWSA dataset

In this study, we have used a combination of various models to estimate TWSA for the pre-GRACE era, back to 1980. Models, from a simple box model to a recent sophisticated deep learning model, have been designed to enhance our understanding and acuity of the Earth's water system that occurs as an exchange between the terrestrial biosphere and atmosphere. In general, three different groups of models have been developed, namely Land Surface Mod-

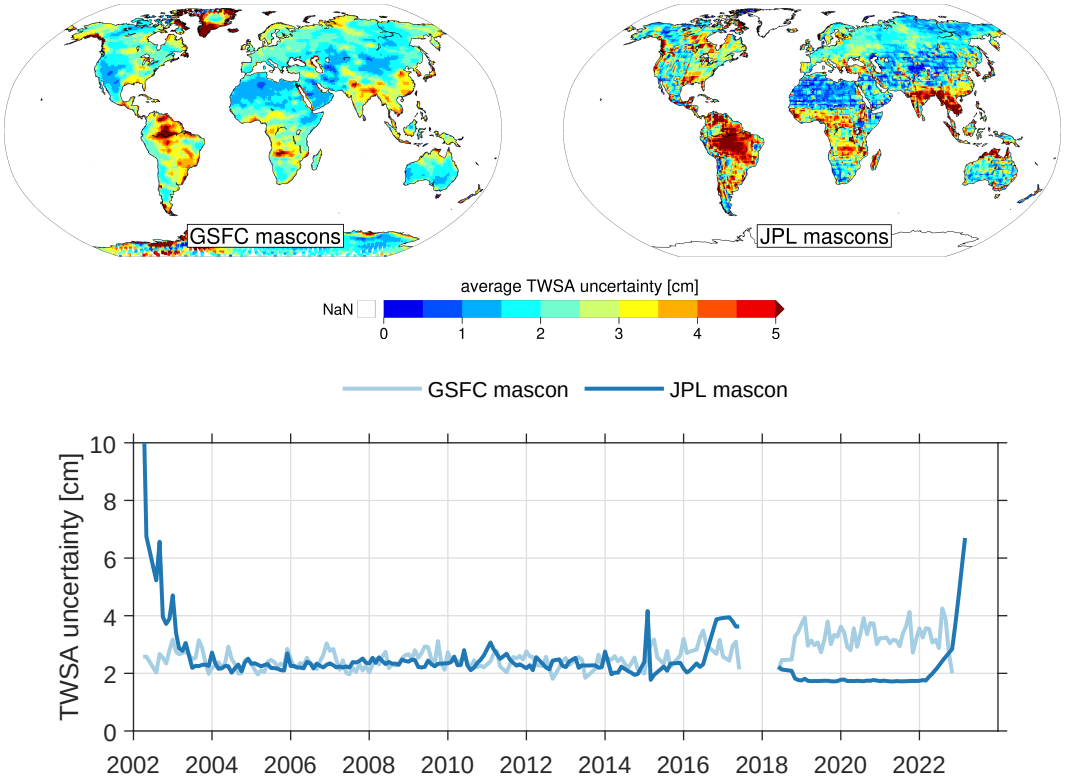

Figure S1. Top: Global distribution of the averaged TWSA uncertainty spanning from April 2002 to November 2022. Bottom: Time series of the global averaged TWSA uncertainty. The data is obtained from two distinct mascon datasets: JPL RL06-v02 and GSFC RL06-v02.

els (LSMs), Global Hydrological Models (GHMs), and global atmospheric reanalysis models. In this study, we have employed in total of 13 state-of-the-art datasets of Global Hydrological Models (GHMs), Land Surface Models (LSMs), and atmospheric reanalysis models (Table S3). Nine multi-decadal global water resources datasets were obtained from the eartH2Observe Water Cycle Integrator (WCI; `ftp://wci.earth2observe.eu` (last access: 31 May 2021)), including PCR-GLOBWB, SURFEX-TRIP, HBV-SIMREG, HTESSEL-CaMa, JULES, LISFLOOD, ORCHIDEE, SWBM, and W3RA. The output of these datasets is available at 0.5 ° spatial resolution over the period 1979–2012. Besides datasets from eartH2Observe, we have included the Community Land Model Version 5 (CLM5) with two standard forcing datasets, namely the Global Soil Wetness Project forcing data set (GSWP3) and CRUNCEP (the combination of the Climate Research Unit (CRU) and the National Centers for Environmental Prediction (NCEP)). The CLM5 datasets are at 0.5 ° spatial resolution covering the period 1901–2014 (for more detail about the CLM5 model, please see Lawrence et al. (2019)). The CLM5 products are accessible via Earth

System Grid (ESG) (Oleson et al., 2019). We have also included the latest version of the WaterGAP Global Hydrology Model (WaterGAP v2.2d) (Müller Schmied et al., 2021), covering the period 1901–2016 and at 0.5 ° spatial resolution. The outputs of the WaterGap v2.d are available at (`https://doi.pangaea.de/10.1594/PANGAEA.918447`). Finally, we have included the fifth generation ECMWF atmospheric reanalysis of the global climate (ERA5) at 0.25 ° spatial resolution which provides data from 1979 to the present. The data is downloaded from the Copernicus Climate Change Service (C3S) at ECMWF (`https://cds.climate.copernicus.eu`)(last access: 30 May 2021). TWSA from models carries a higher spatial resolution and therefore values with higher frequency. To set the same spectral content in models compared to GRACE TWSA, we have transferred the model outputs into the spectral domain and truncated the SHs to the maximum degree and order 96. Finally, we recovered the TWSA fields from the truncated SHs.

Table S3. Summary of global models used in this study. GHM: Global Hydrological Model; LSM: Land Surface Model; ReA: Reanalysis Model.

	Model	Time Period	Data Provider	Reference
GHM	WGHM	1901–2016	Goethe University Frankfurt	Müller Schmied et al. (2021)
	PCRGLOB-WB	1979–2012	Utrecht University (UU)	Wada et al. (2014)
				Sutanudjaja et al. (2018)
	HBV-SIMREG	1979–2012	Joint Research Centre (JRC)	Lindström et al. (1997)
	LISFLOOD	1979–2012	Joint Research Centre (JRC)	Van Der Knijff et al. (2010)
	W3RA	1979–2012	CSIRO**	Van Dijk (2010)
	SWBM	1979–2012	Simple Water Balance Model	Koster & Mahanama (2012)
				Orth & Seneviratne (2013)
LSM	CLM5	1940–2014	The Earth System Grid (ESG) at NCAR	Lawrence et al. (2019)
	HTESSEL	1979–2012	ECMWF	Balsamo et al. (2015)
	JULES	1979–2012	Centre for Ecology and Hydrology (CEH)	Best et al. (2011)
				Clark et al. (2011)
	ORCHIDEE	1979–2012	French National Centre for Scientific Research	Polcher et al. (2011)
	SURFEX-TRIP	1979–2012	Meteo France	Decharme et al. (2013)
ReA	ERA5	1979–2016	ECMWF*	Hersbach et al. (2020)

* ECMWF: European Centre for Medium-Range Weather Forecasts

** CSIRO: Commonwealth Scientific and Industrial Research Organisation

2.1 Multivariate Linear Regression

To combine models, we have used the Multivariate Linear Regression (MLR) method. MLR is a statistical method used for estimating the parameters of a linear regression model with multiple independent variables. MLR has several advantages, including its ability to handle multiple independent variables and to model complex relationships between variables. It also provides estimates of the coefficients and their standard errors, which can be used to test hypotheses and construct confidence intervals. However, MLR assumes that the errors are normally distributed and have constant variance, which may not always be true in practice. Additionally, it can be sensitive to outliers and multicollinearity among the independent variables. The basic idea behind MLR is to find the coefficients that minimize the sum of squared errors between the predicted and actual values of the dependent variable. The formula for MLR is as follows:

$$\mathbf{y} = \mathbf{X}\boldsymbol{\beta} + \boldsymbol{\epsilon} \tag{1}$$

Here $\mathbf{y}$ is the vector of dependent variable values, $\mathbf{X}$ is the matrix of independent variable values, $\boldsymbol{\beta}$ is the vector of coefficients to be estimated, and $\boldsymbol{\epsilon}$ is the vector of errors, which are assumed to be normally distributed with mean zero and constant variance.

2.2 Compare with GRACE

To evaluate the performance of the long-term TWSA dataset from the MLR method ($\mathrm{TWSA_{MLR}}$), we have compared the results with GRACE estimation within the GRACE era (April 2002 to December 2012).

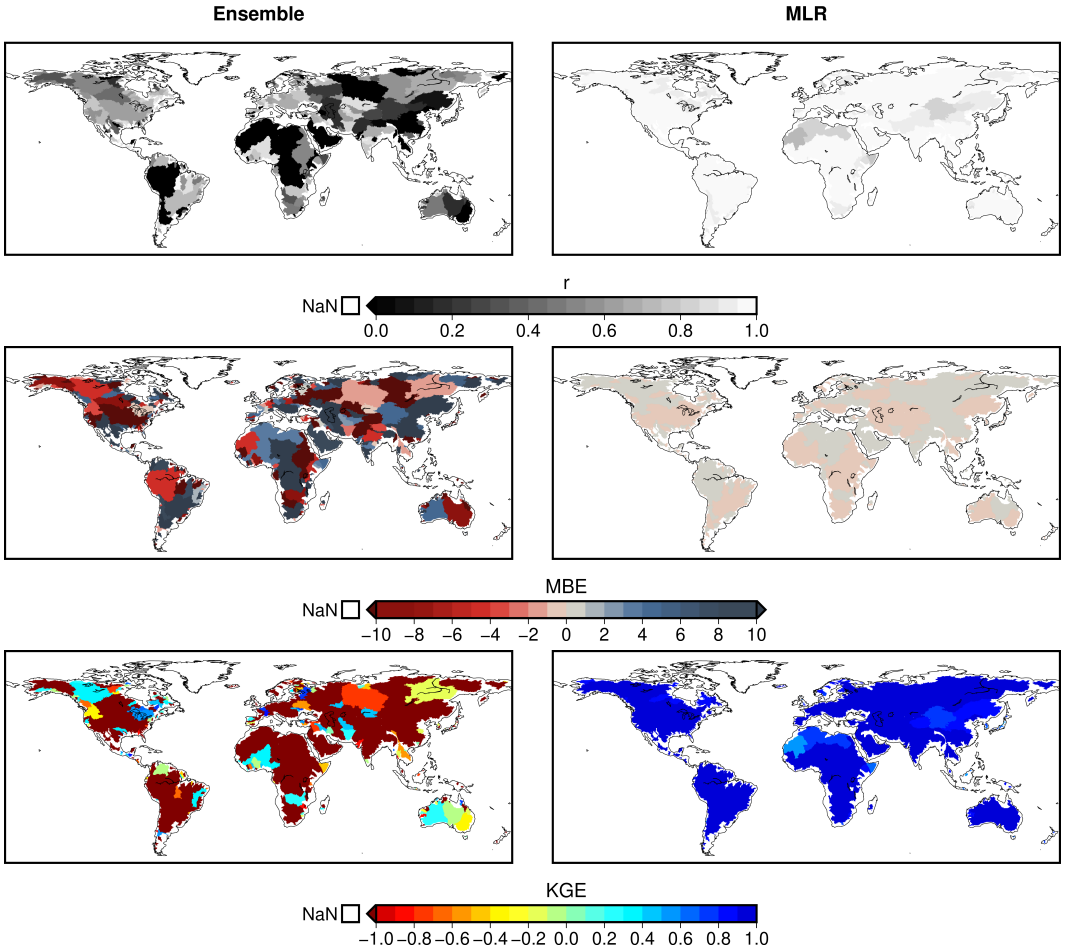

Figure S2. Global distribution of the correlation coefficient (r), Mean Bias Error (MBE), and Kling-Gupta Efficiency (KGE) values for major river basins (excluding Greenland and Antarctica) obtained from the comparison between the reconstructed TWSA from ensemble mean and Multivariate Linear Regression (MLR) and GRACE during 2003–2012.

3 Handling trends

Several studies have suggested that before investigating drought indices using the GRACE TWSA time series, detrending is necessary (e.g., Liu et al., 2020; Khorrami & Gunduz, 2021). Liu et al. (2020), for instance, have demonstrated that without detrending TWSA time series drought severity can be overestimated over some basins in China after 2013. While the soil moisture data suggests that the drought ceased in September 2014, their GRACE indices (GRACE-DSI) show a continuous drought condition. In contrast to the aforementioned studies, we deliberately retain the trend in the time series. We reason that the trend

reflects long-term changes in climate, such as temperature increases or precipitation pattern alterations, which can affect the frequency and severity of droughts. Eliminating the trend would essentially omit these long-term changes from the analysis, providing an incomplete understanding of the hydrological system.

To demonstrate the impact of detrending, we calculated the TWSA time series in two real cases using the SSA approach with a 24-month window to remove the trend in the data. The two cases, the Tigris basin in the Middle East with a negative trend and the Niger basin in Africa with a positive trend are presented in Figure S3 and Figure S4, respectively. In each case, we compared the results from two scenarios: one without detrending, denoted by the solid line in (c) and (d) and labeled as (a), and one with detrending, shown as the dashed line in (c) and (e) and labeled as (b).

The Tigris basin experienced a prolonged period of water loss, particularly after 2007, which is apparent in the red area in Figure S3(d). Detrending the data resulted in higher values for the climatology compared to the non-detrended data, as shown in Figure S3(c), and caused oscillations between wet and dry years, as seen in Figure S3(e). On the other hand, the Niger basin exhibited a positive trend mainly after 2010, resulting in wetter years in the basin, as depicted in Figure S4(d). Although detrending did not significantly alter the climatology, as illustrated in Figure S4(c), it did reveal dry years after 2010, which is inconsistent with actual conditions.

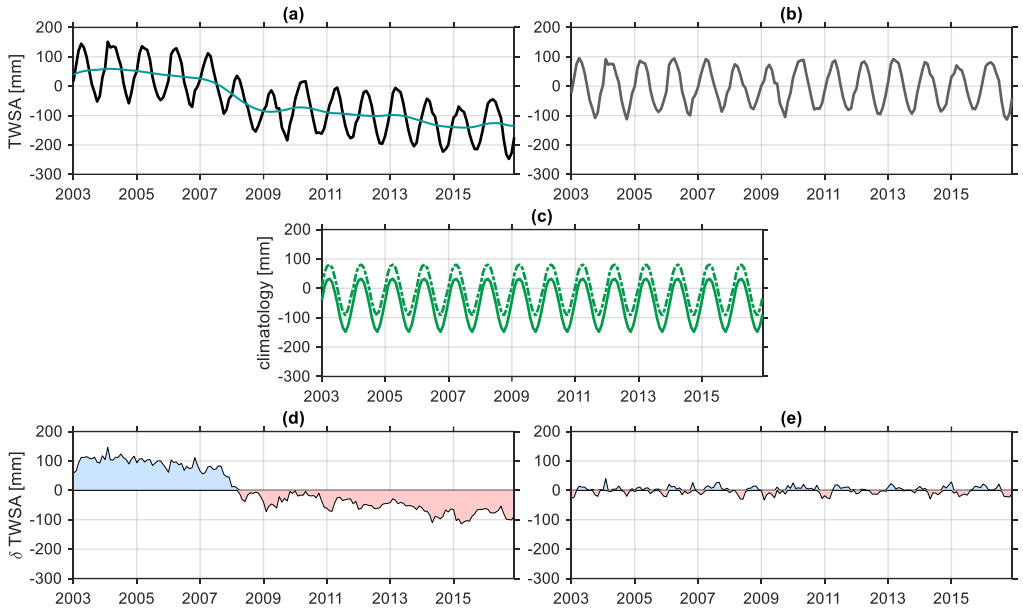

Figure S3. This figure presents a comprehensive analysis of TWSA for the Tigris River basin in the Middle East, using data from GRACE satellite mission. (a) shows the time series of TWSA from GRACE, along with its inter-annual variations which are extracted using the Singular Spectrum Analysis (SSA) approach with a 24-month window. (b) displays the TWSA after removing the inter-annual variations, highlighting the long-term trends. (c) illustrates the climatology of TWSA, which represents the long-term monthly mean. The solid and dashed lines represent the climatology obtained from (a) and (b), respectively. (d) and (e) show the TWSA residuals, obtained by subtracting the corresponding climatology from panels (a) and (b), respectively. These residual plots reveal the short-term fluctuations in TWSA that are not captured by the climatology.

4 Major river basins

In this study, we have presented and analyzed the results of the global major river basins. The border of the basins follows the HydroSHEDS database (`https://www.hydrosheds.org/`). Moreover, the climate of the basins is determined using the Aridity Index (AI), which is the ratio of total annual precipitation to potential evapotranspiration. To compute the aridity index, we have employed the latest version of the European Center for Medium-Range Weather Forecasts (ECMWF) Reanalysis (ERA), namely ERA5 (Hersbach et al., 2020). Based on AI, the climate of the basins can be categorized into humid (AI $>$ 0.65), sub-humid (AI $\leq$ 0.65, and AI $>$ 0.5), semi-arid (AI $\leq$ 0.5 and $>$ 0.2), arid (AI $\leq$ 0.2 and $>$ 0.05), and hyperarid (AI $\leq$ 0.05). This study grouped arid and hyper-arid into one group,

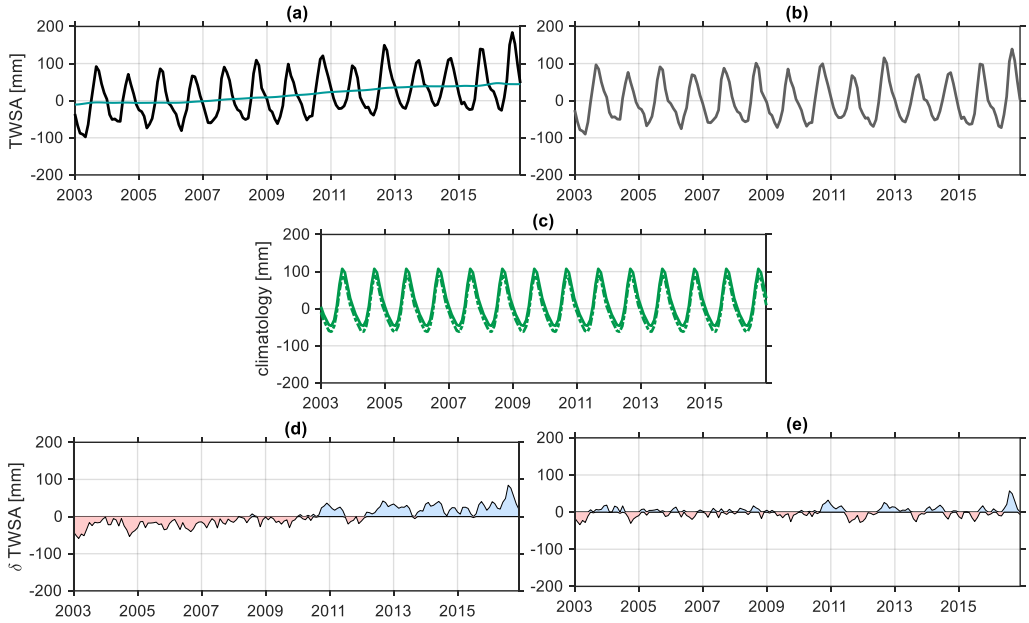

Figure S4. Same as Figure S3 but for Niger river basin in West Africa, flowing through 10 countries: Guinea, Mali, Niger, Benin, Burkina Faso, Cote d'Ivoire, Ghana, Togo, Cameroon, and Nigeria.

Arid-hyper Arid (Figure S5). Based on AI criteria, 60 % of the river basins are categorized as humid, $\sim$ 10 % as sub-humid, 22 d% as semiarid, and $\sim$ 8 % as arid to hyper-arid).

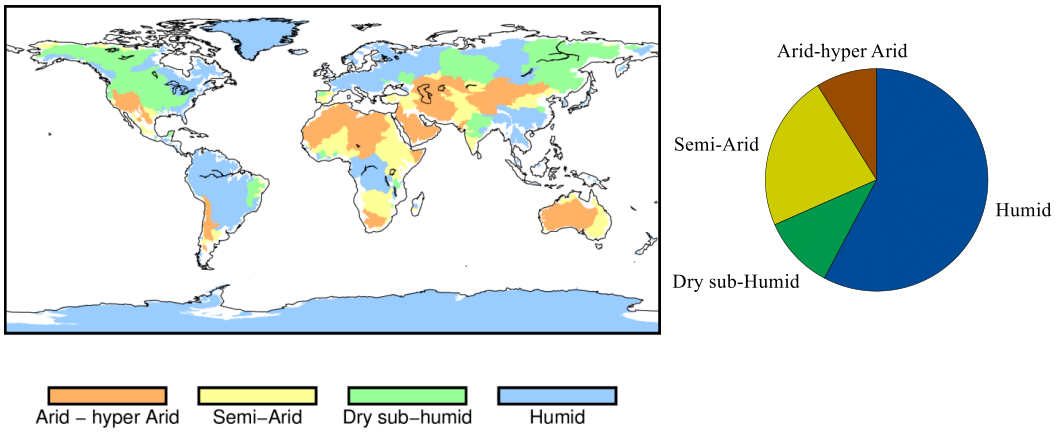

Figure S5. Global distribution of the major river basins together with their corresponding climate category. Besides, a pie chart illustrates the worldwide share of each category in terms of area.

References

Balsamo, G., Albergel, C., Beljaars, A., Boussetta, S., Brun, E., Cloke, H., ... others (2015). ERA-Interim/Land: a global land surface reanalysis data set. *Hydrology and Earth System Sciences*, *19*(1), 389–407. doi: 10.5194/hess-19-389-2015

Bandikova, T., McCullough, C., Kruizinga, G. L., Save, H., & Christophe, B. (2019). GRACE accelerometer data transplant. *Advances in Space Research*, *64*(3), 623–644.

Best, M., Pryor, M., Clark, D., Rooney, G., Essery, R., Ménard, C., ... others (2011). The Joint UK Land Environment Simulator (JULES), model description–Part 1: energy and water fluxes. *Geoscientific Model Development*, *4*(3), 677–699. doi: 10.5194/gmd-4-677-2011

Clark, D., Mercado, L., Sitch, S., Jones, C., Gedney, N., Best, M., ... others (2011). The Joint UK Land Environment Simulator (JULES), model description–Part 2: carbon fluxes and vegetation dynamics. *Geoscientific Model Development*, *4*(3), 701–722. doi: 10.5194/gmd-4-701-2011

Decharme, B., Martin, E., & Faroux, S. (2013). Reconciling soil thermal and hydrological lower boundary conditions in land surface models. *Journal of Geophysical Research: Atmospheres*, *118*(14), 7819–7834. doi: 10.1002/jgrd.50631

Hersbach, H., Bell, B., Berrisford, P., Hirahara, S., Horányi, A., Muñoz-Sabater, J., ... others (2020). The ERA5 global reanalysis. *Quarterly Journal of the Royal Meteorological*

Society, *146*(730), 1999–2049. doi: 10.1002/qj.3803

Khorrami, B., & Gunduz, O. (2021). An enhanced water storage deficit index (EWSDI) for drought detection using GRACE gravity estimates. *Journal of Hydrology*, *603*, 126812. doi: 10.1016/j.jhydrol.2021.126812

Koster, R. D., & Mahanama, S. P. (2012). Land surface controls on hydroclimatic means and variability. *Journal of Hydrometeorology*, *13*(5), 1604–1620. doi: 10.1175/JHM-D-12-050.1

Landerer, F., Flechtner, F. M., Save, H., Webb, F. H., Bandikova, T., Bertiger, W. I., ... others (2020). Extending the global mass change data record: GRACE Follow-On instrument and science data performance. *Geophysical Research Letters*, *47*(12), e2020GL088306. doi: 10.1029/2020GL088306

Lawrence, D. M., Fisher, R. A., Koven, C. D., Oleson, K. W., Swenson, S. C., Bonan, G., ... others (2019). The Community Land Model version 5: Description of new features, benchmarking, and impact of forcing uncertainty. *Journal of Advances in Modeling Earth Systems*, *11*(12), 4245–4287. doi: 10.1029/2018MS001583

Lindström, G., Johansson, B., Persson, M., Gardelin, M., & Bergström, S. (1997). Development and test of the distributed HBV-96 hydrological model. *Journal of hydrology*, *201*(1-4), 272–288. doi: 10.1016/S0022-1694(97)00041-3

Liu, X., Feng, X., Ciais, P., Fu, B., Hu, B., & Sun, Z. (2020). GRACE satellite-based drought index indicating increased impact of drought over major basins in China during 2002–2017. *Agricultural and Forest Meteorology*, *291*, 108057. doi: 10.1016/j.agrformet.2020.108057

Loomis, B., Luthcke, S., & Sabaka, T. (2019). Regularization and error characterization of GRACE mascons. *Journal of geodesy*, *93*(9), 1381–1398. doi: 10.1007/s00190-019-01252-y

Mayer-Gürr, T., Behzadpour, S., Kvas, A., Ellmer, M., Klinger, B., Strasser, S., & Zehentner, N. (2018). ITSG-Grace2018: Monthly, Daily and Static Gravity Field Solutions from GRACE. *Graz University of Technology*. doi: 10.5880/ICGEM.2018.003

Müller Schmied, H., Cáceres, D., Eisner, S., Flörke, M., Herbert, C., Niemann, C., ... others (2021). The global water resources and use model WaterGAP v2. 2d: Model description and evaluation. *Geoscientific Model Development*, *14*(2), 1037–1079. doi: 10.5194/gmd-14-1037-2021

Oleson, K., Lawrence, D., Lombardozzi, D., & Wieder, D. (2019). *CLM land-only release.* (Accessed: 2021-05-30) doi: https://doi.org/10.5065/d6154fwh

Orth, R., & Seneviratne, S. I. (2013). Predictability of soil moisture and streamflow on subseasonal timescales: A case study. *Journal of Geophysical Research: Atmospheres*, *118*(19), 10–963. doi: 10.1002/jgrd.50846,2013

Polcher, J., Bertrand, N., Biemans, H., Clark, D. B., Floerke, M., Gedney, N., ... Voss, F. (2011). Improvements in hydrological processes in general hydrological models and land surface models within WATCH.

Save, H. (2016). Grace battery status and science impact. In *Grace science team meeting, potsdam, germany oct* (pp. 5–7).

Scanlon, B. R., Zhang, Z., Save, H., Wiese, D. N., Landerer, F. W., Long, D., ... Chen, J. (2016). Global evaluation of new GRACE mascon products for hydrologic applications. *Water Resources Research*, *52*(12), 9412–9429. doi: 10.1002/2016WR019494

Sutanudjaja, E. H., Van Beek, R., Wanders, N., Wada, Y., Bosmans, J. H., Drost, N., ... others (2018). PCR-GLOBWB 2: a 5 arcmin global hydrological and water resources model. *Geoscientific Model Development*, *11*(6), 2429–2453. doi: 10.5194/gmd-11-2429-2018

Van Der Knijff, J., Younis, J., & De Roo, A. (2010). LISFLOOD: a GIS-based distributed model for river basin scale water balance and flood simulation. *International Journal of Geographical Information Science*, *24*(2), 189–212. doi: 10.1080/13658810802549154

Van Dijk, A. (2010). The Australian Water Resources Assessment System Technical Report 3. Landscape Model (version 0.5) Technical Description.
doi: 10.4225/08/5852dd9bb578c

Wada, Y., Wisser, D., & Bierkens, M. F. (2014). Global modeling of withdrawal, allocation and consumptive use of surface water and groundwater resources. *Earth System Dynamics*, *5*(1), 15–40. doi: 10.5194/esd-5-15-2014

Wahr, J., Molenaar, M., & Bryan, F. (1998). Time variability of the Earth's gravity field: Hydrological and oceanic effects and their possible detection using GRACE. *Journal of Geophysical Research: Solid Earth*, *103*(B12), 30205–30229. doi: 10.1029/98JB02844

Watkins, M. M., Wiese, D. N., Yuan, D.-N., Boening, C., & Landerer, F. W. (2015a). Improved methods for observing Earth's time variable mass distribution with GRACE using spherical cap mascons. *Journal of Geophysical Research: Solid Earth*, *120*(4), 2648–2671. doi: 10.1002/2014JB011547

Watkins, M. M., Wiese, D. N., Yuan, D.-N., Boening, C., & Landerer, F. W. (2015b). Improved methods for observing Earth's time variable mass distribution with GRACE

using spherical cap mascons. *Journal of Geophysical Research: Solid Earth*, *120*(4), 2648–2671. doi: 10.1002/2014JB011547

Wiese, D., Landerer, F. W., & Watkins, M. M. (2016). Quantifying and reducing leakage errors in the JPL RL05M GRACE mascon solution. *Water Resources Research*, *52*(9), 7490–7502. doi: 10.1002/2016WR019344

Wiese, D., Yuan, D., Boening, C., Landerer, F., & Watkins, M. (2018). JPL GRACE mascon ocean, ice, and hydrology equivalent water height release 06 coastal resolution improvement (CRI) filtered version 1.0. *DAAC: Pasadena, CA, USA*. (Last accessed: 1 February 2021) doi: 10.5067/TEMSC-3MJC6

Wiese, D. N., Landerer, F. W., & Watkins, M. M. (2016). Quantifying and reducing leakage errors in the JPL RL05M GRACE mascon solution. *Water Resources Research*, *52*(9), 7490–7502. doi: 10.1002/2016WR019344